Optical Coherence Tomographic Correlates of Angiographic Subtypes of Occult Choroidal Neovascularization

Amirhossein Hariri,[1] Florian M. Heussen,[1,2] Muneeswar Gupta Nittala,[1] and SriniVas R. Sadda[1,3]

[1]Doheny Eye Institute, Los Angeles, California
[2]Department of Ophthalmology, Charité, University Medicine, Berlin, Germany
[3]Department of Ophthalmology, Keck School of Medicine of the University of Southern California, Los Angeles, California

Correspondence: SriniVas R. Sadda, Doheny Eye Institute, 1450 San Pablo Street, Los Angeles, CA 90033; SSadda@doheny.org.

Submitted: April 27, 2013
Accepted: October 28, 2013

Citation: Hariri A, Heussen FM, Nittala MG, Sadda SR. Optical coherence tomographic correlates of angiographic subtypes of occult choroidal neovascularization. *Invest Ophthalmol Vis Sci*. 2013;54:8020–8026. DOI:10.1167/iovs.13-12302

Purpose. To compare the optical coherence tomographic (OCT) correlates of two previously described angiographic subtypes of occult choroidal neovascularization (CNV).

Methods. We retrospectively analyzed 17 consecutive patients with previously untreated occult CNV who underwent both fluorescein angiography (FA) and volume spectral domain (SD)-OCT imaging on the same visit. Planimetric grading was performed on the FA images by certified reading center graders to precisely outline the boundaries of the fibrovascular pigment epithelial detachment (FVPED) and/or late leakage of undetermined source (LLUS) components of occult CNV for each case. In the SD-OCT images, the outer retinal pigment epithelial (RPE) and inner choroidal boundaries were manually segmented on all B-scans to generate a PED thickness map. Fluorescein angiography images were manually registered with the OCT fundus image, and the PED thickness was correlated with the angiographic lesion component present at each corresponding point in the fundus.

Results. Point-to-point correlations revealed that PED thickness was significantly different in areas of FVPED versus areas of LLUS. Whereas the mean PED thickness in areas of FVPED was 196.1 ± 120.36 μm, it was only 38.42 ± 8.14 μm in areas of LLUS ($P = 0.003$). Normalized internal reflectivity in areas of FVPED was lower than in areas of LLUS (0.12 ± 0.11 vs. 0.24 ± 0.07; $P = 0.03$). The integrity or continuity of the overlying RPE band on OCT, however, did not appear to differ between areas of LLUS and FVPED ($P = 0.33$).

Conclusions. Although LLUS and FVPED appear to be distinct angiographic subtypes of CNV, the major difference between the two is the height of the RPE elevation and the internal reflectivity, with areas of LLUS representing much shallower RPE elevations with brighter mean internal reflectivity.

Keywords: occult choroidal neovascularization, fibrovascular pigment epithelial detachment, late leakage of undetermined source, optical coherence tomography

Historically, occult choroidal neovascularization (CNV) has been classified as one of two types, fibrovascular pigment epithelial detachment (FVPED) or late leakage of undetermined source (LLUS). These subtypes of occult CNV are differentiated on the basis of stereoscopic fluorescein angiography (FA). FVPEDs correspond to areas of retinal pigment epithelium (RPE) elevation with stippled hyperfluorescence, which can be well demarcated with varying degrees of early brightness (depending on the extent of the overlying RPE depigmentation), with staining and moderate leakage in the mid-late phases. In contrast to FVPED (and in contrast to classic CNV), LLUS does not demonstrate early hyperfluorescence, manifesting instead as late-appearing, speckled hyperfluorescence with pooling of dye in the overlying neurosensory space. The boundaries of this subtype of occult CNV are never well demarcated.[1]

Because of its late appearance and poor demarcation, LLUS can prove challenging to reliably detect and distinguish, and some investigators have expressed skepticism as to whether it should be considered a distinct entity. The advent of optical coherence tomography (OCT), in particular spectral domain (SD)-OCT with high-resolution cross-sectional imaging of the subretinal and sub-RPE space, has provided an opportunity to study CNV lesions from a different perspective than that of traditional angiography. Many groups, including ours, have correlated OCT and FA findings in CNV lesions and have demonstrated that occult CNV generally corresponds to areas of PED on OCT.[2] The OCT correlates of the specific subtypes of occult CNV, however, have not been defined. In the present study, we used detailed subanalysis and point-to-point correlation between high-resolution SD-OCT and angiography to elucidate the differences between the angiographic subtypes of occult CNV.

Materials and Methods

We retrospectively reviewed the University of Southern California Department of Ophthalmology medical records between 2007 and 2009 to identify consecutive cases of patients with neovascular age-related macular degeneration

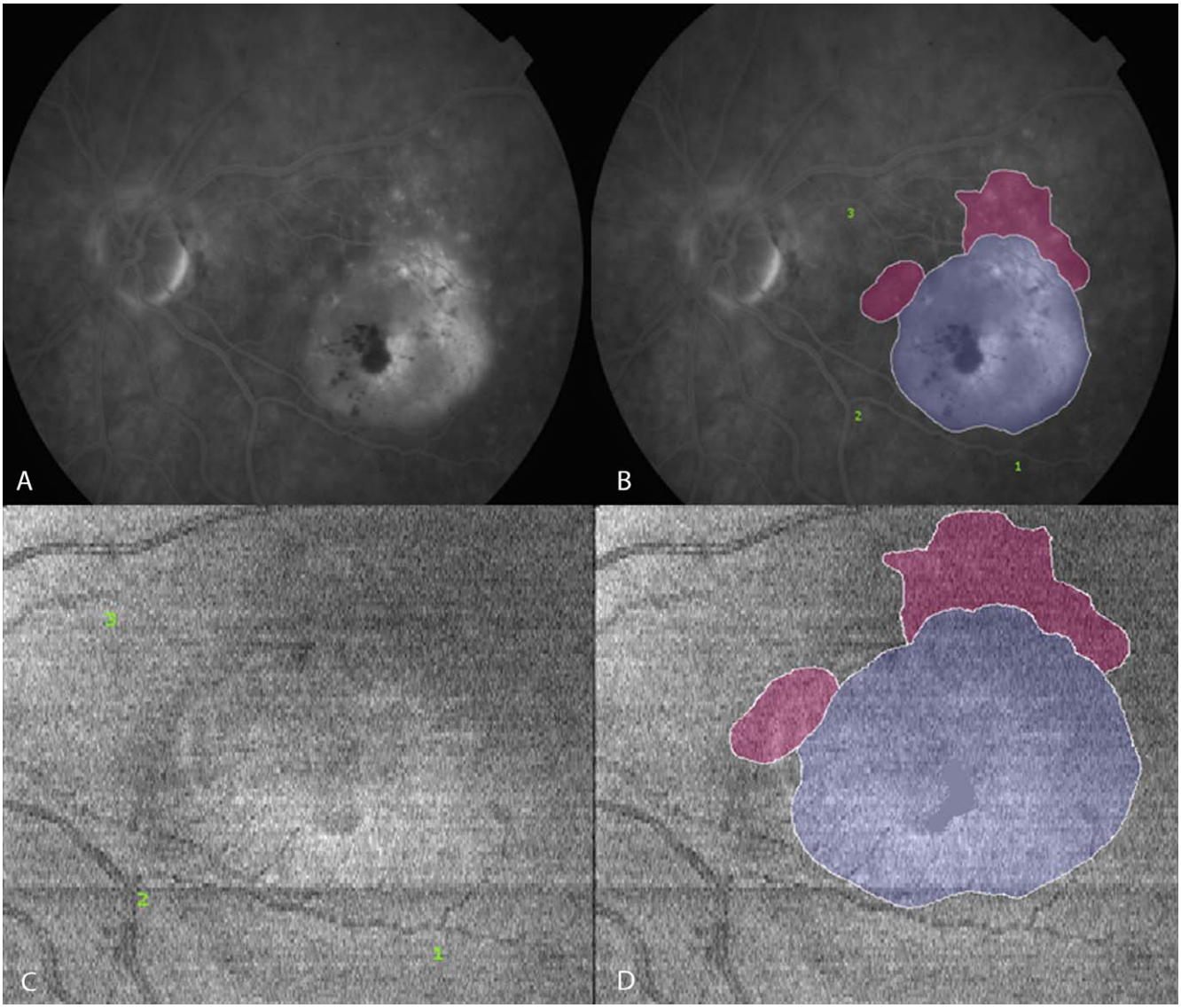

FIGURE 1. (**A**) Late-phase FA image illustrating occult choroidal neovascularization. The reading center grader manually segmented the lesion (**B**) into areas of LLUS (*magenta*) and FVPED. The OCT projection image (**C**) allows the vascular landmarks to be readily seen. Marking of at least three corresponding vessel points (1, 2, 3) in the FA and OCT projection images allows them to be registered to one another by the reading center grading software. The registered image showing the FA annotation superimposed on the OCT projection image is shown in (**D**). The registration technique adjusts for differences in scale and aspect ratio.

(AMD) prior to treatment who underwent both SD-OCT and FA on the same day and who were noted by the treating physician to have occult with no classic CNV on FA. Volume SD-OCT images were obtained using a Cirrus HD OCT (Carl Zeiss Meditec, Dublin, CA) or Topcon 3D OCT-2000 (Topcon, Tokyo, Japan) with a 512 × 128 macular cube acquisition protocol. Stereoscopic color fundus photographs and FA were obtained using a Topcon TRC-50DX (Topcon Medical Systems, Paramus, NJ). Lesion classification was confirmed by inspection of the FA images by two trained reading center graders (AH and FMH) before inclusion in the study. Choroidal neovascularization resulting from pathologies other than AMD, the presence of other retinal pathology, or poor OCT image quality that would degrade confidence in grading (specifically, a signal strength less than 7 with the Cirrus OCT or an image quality score less than 70 with the Topcon OCT) were criteria for exclusion. The study was approved by the institutional review board of the University of Southern California, and the research adhered to the tenets set forth in the Declaration of Helsinki. Seventeen eyes of 17 patients met the inclusion criteria and were included. Images were exported for masked review at the reading center by a CNV-grading certified angiography and OCT grader (FMH). The OCT and FA images were graded separately in a masked fashion. In addition, all grading was repeated by a second independent masked grader (AH). Despite the fact that our group has had several prior publications about reproducibility in grading of CNV lesions on FA and OCT,[3,4] in this particular study again all cases, not only those with discrepancies or queries, were rereviewed by the medical director of the Doheny Image Reading Center (SRS), who served as the final arbitrator for all cases. The summary statistics and comparisons between areas of LLUS and FVPED are based only on this final arbitrated result.

Angiographic images were loaded into GRADOR, a custom image viewing and planimetric grading software program developed by the Doheny Image Reading Center; this software

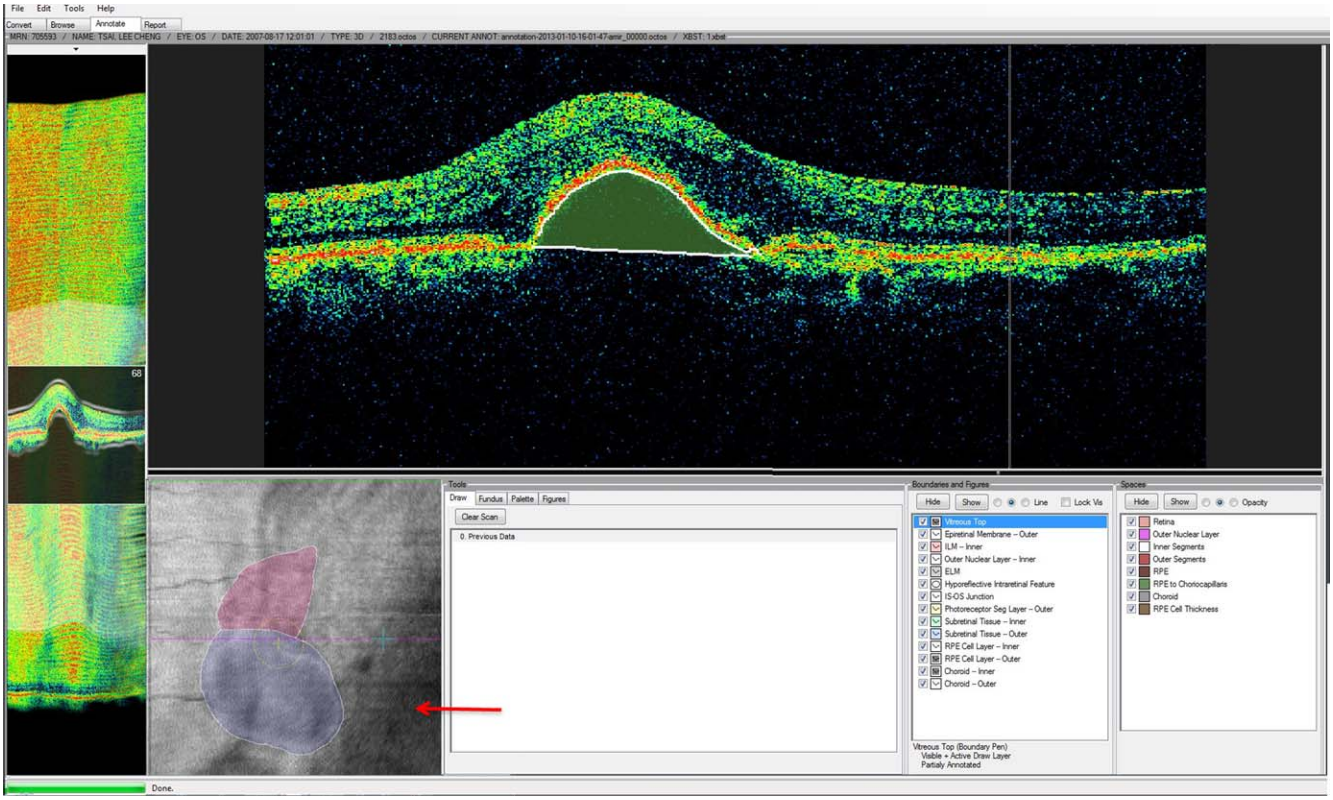

Figure 2. Illustration of the OCTOR reading center software graphical user interface. The borders of the PED on the OCT B-scan have been manually traced by the grader. The annotations (*outline of the CNV lesion*) from the fluorescein angiogram have been subsequently registered onto the OCT projection image (*arrow*), which is displayed at the *bottom* of the interface. By clicking in either the projection image window or the B-scan window, the user is able to quickly correlate between the OCT and FA findings.

has already been validated.[4] The software allows stereoscopic viewing of image pairs and classification of lesions and delineation of lesion boundaries. Once the boundaries are delineated, the software allows automatic calculation of various quantitative parameters, such as the number and size of lesions. For the purpose of this study, only the borders of the occult components of the CNV lesion were drawn by the graders; other lesion components, such as contiguous thick blood or blocked fluorescence, were not included. In accordance with definitions from previous clinical trials of CNV, the borders of the occult CNV lesion were drawn on the late FA frames 5 minutes after dye injection.

The occult CNV was subdivided into FVPED and LLUS. FVPED was identified as areas of irregular RPE elevation and stippled hyperfluorescence, typically with well-demarcated borders that were clearly visible by the midphase of the FA, demonstrating overlying leakage in the late frames. In contrast, LLUS was recognized as late-appearing areas of deep leakage that did not correspond to areas of RPE elevation. The foveal center was also marked by the grader.

The OCT volume cubes were exported from the instruments and loaded into 3D-OCTOR, version 3, a custom OCT grading software program developed by the Doheny Image Reading Center that has previously been described and validated.[3,5] Manual segmentation and grading of various CNV lesion components (PED, subretinal fluid, subretinal tissue, and so on) have been described in previous reports, and intergrader reproducibility has been shown to be high.[3] From previous studies, occult CNV on FA was shown to correspond to vascularized PED visible on OCT.[2] To quantify the PED for this analysis, the graders manually segmented the outer RPE surface and the inner border of the choroid/Bruch's membrane along the entire length of the B-scan for each of the B-scans in the volume cube. The software then computed the vertical distances between the boundaries (for every A-scan) and interpolated between adjacent B-scans to generate thickness maps for the PED and all other segmented structures of interest, analogous to maps provided by the instrument software. For this study, the mean thickness of the PED was the parameter used to compare areas of LLUS and FVPED. Previously, we have demonstrated that drusenoid PEDs can be distinguished from vascularized PEDs on OCT based on their internal reflectivity (homogenous for drusen versus heterogenous for vascularized PED).[6] These qualitative assessments of PEDs have been further validated by phase variance OCT analysis, in which vessels can be demonstrated within these vascularized PEDs (Sadda SR, unpublished observations, 2013). For this analysis, we included areas of homogenous drusen/drusenoid PEDs within the PED segmentation.

To correlate the OCT-derived CNV lesion thickness maps with the planimetric angiographic grading, the OCT and FA were registered. To register the datasets, the OCT projection map was exported from 3D-OCTOR and imported into GRADOR for semiautomatic registration. Retinal vessel crossing points (minimum three required) were used as invariant landmarks for image alignment (Fig. 1). Once the OCT and FA data were aligned, the portions of the OCT volume cube corresponding to the LLUS and FVPED components on FA could be separately analyzed and quantified (Fig. 2). In addition to thickness, mean internal reflectivity (MIR) of the PED was calculated. To account for variable image brightness in different images, as in previous reports,[6] we compared optical density ratios (ODR) rather than non-normalized internal reflectivities. The brightness of PED was normalized by

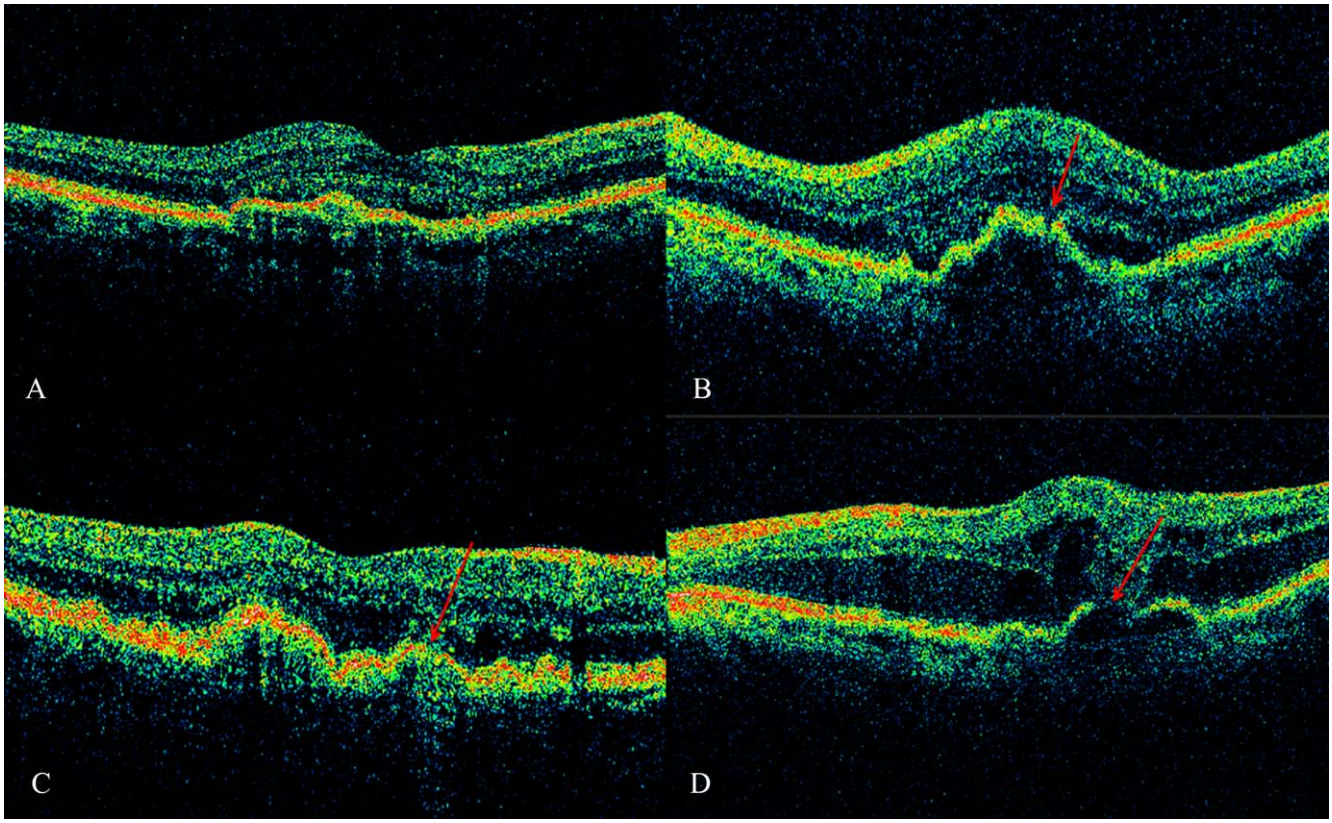

FIGURE 3. (**A–D**) Illustrations of examples of different extents of discontinuity encountered in individual B-scans while grading the severity of RPE disruption in regions of angiographic occult CNV. *Red arrows* indicate the area of RPE disruption. (**A**) Continuous: normal-appearing band with normal reflectivity. (**B**) Questionably disrupted: Variations in the reflectivity or brightness of the RPE band are present, but no actual disruption (gap in the band) is observed. (**C**) The sum of all pixels in which the RPE band is discontinuous is more than 1 but less than 5 pixels. (**D**) The summed extent of discontinuity in the RPE band is more than 5 pixels.

comparing it with two reference structures that are not expected to be affected by the disease process: the vitreous and the nerve fiber layer (NFL). To calculate the ODR of the PED areas of interest, we subtracted the mean intensity of the vitreous from mean internal reflectivity of the PED and divided the result by the mean internal reflectivity of NFL: ODR of PED = (MIR of PED − MIR of vitreous)/MIR of NFL.

In this series, subretinal tissue (i.e., hyperreflective material above the RPE) was not present in the areas corresponding to the occult CNV and thus was not included in further analyses.

In addition to quantitative comparisons, the integrity of the RPE band in areas of LLUS and FVPED was assessed on a qualitative, categorical scale from 0 to 4. For this assessment, we considered only those portions of the RPE band on OCT that were noted to fall within areas of occult CNV as determined by FA (note that graders were masked as to whether the particular area was LLUS or FVPED). Overlay maps of the angiogram on the OCT projection image (Fig. 2) were used to aid the grader in determining the region of occult CNV. The percentage of the RPE band that was discontinuous within this region was then estimated and classified into broad categories as follows:

0. Normal: no discontinuity;
1. Questionable: discontinuity less than 10%;
2. Mild: discontinuity more than 10% but less than 33%;
3. Moderate: discontinuity more than 33% but less than 66%; and
4. Severe: discontinuity more than 66%.

Figure 3 illustrates examples of different types of discontinuity encountered when grading the severity of RPE disruption in areas of occult CNV. In making their determinations, graders also considered the impact of shadowing from overlying intraretinal hyperreflective material.

A Student's *t*-test was used to compare the thickness and reflectivity of the PED in areas of LLUS or FVPED. The integrity of the RPE in areas of LLUS and FVPED was compared using a χ^2 test. Significance was set at a $P < 0.05$ for both tests. Intraclass correlation coefficients, Bland-Altman plot, and interrater agreement (κ) were used to compare reproducibility of different gradings. Statistical analyses of the data were performed using commercial software (Statistical Package for Social Science, version 19.0; SPSS, Inc., Armonk, NY, and MedCalc, version 12; MedCalc software bvba, Mariakerke, Belgium).

RESULTS

We retrospectively analyzed 17 eyes of 17 consecutive patients with previously untreated occult with no classic CNV who underwent both FA and volume SD-OCT imaging at the same visit.

After detailed grading of the occult CNV lesion by FA, seven eyes were noted to have exclusively LLUS, three had only FVPED, and seven had both LLUS and FVPED components. The areas of the LLUS and FVPED determined by the two graders showed good agreement, with an intraclass correlation coefficient of 0.92 (95% confidence interval [CI]: 0.78–0.97)

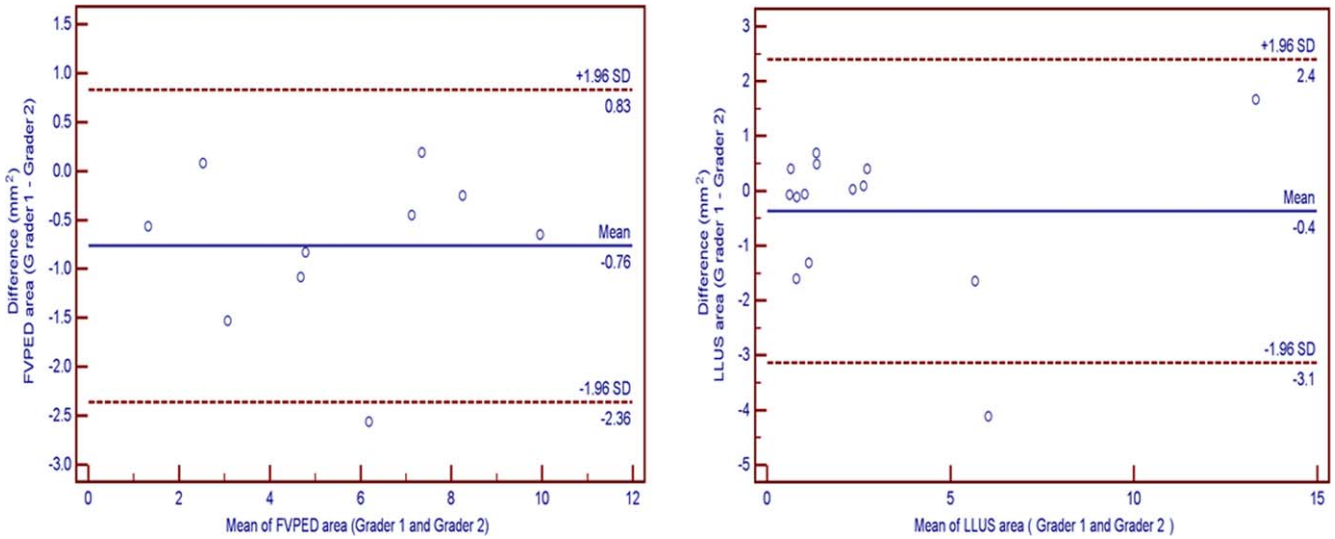

Figure 4. Bland-Altman plots illustrating the level of agreement between graders in measurement of areas of FVPED and LLUS.

in LLUS areas and 0.92 (95% CI: 0.74–0.98) in FVPED areas. The level of agreement is also illustrated in the Bland-Altman plots in Figure 4.

The mean PED thickness on OCT in eyes with LLUS only was 40.4 ± 9.57 μm compared to 234.23 ± 101.52 μm in eyes with both LLUS and FVPED and 75.3 ± 21.43 in eyes with FVPED only. The mean PED area on OCT for all cases combined was significantly smaller than the occult CNV area defined by FA (3.79 ± 3.38 vs. 6.61 ± 5.21 mm^2; $P = 0.008$).

After registration of OCT and FA data and isolation of the portions of the PED corresponding to the areas of FVPED versus LLUS, the mean PED thickness for all cases combined in areas of LLUS was 38.42 ± 8.14 vs. 196.1 ± 120.36 μm for FVPED. This difference was statistically significant ($P = 0.003$, Student's *t*-test). The PED thickness in number of pixels for all A-scans within areas of LLUS and FVPED was also plotted and compared (Fig. 5). The distribution maps illustrate overlap of LLUS and FVPED at shallow PED thicknesses; but at points with thicknesses greater than 50 pixels, a FVPED was nearly always present. Similarly, PED volume differed significantly ($P = 0.009$) between areas of LLUS (0.16 ± 0.29 mm^3) and FVPED (1.263 ± 1.03 mm^3). Although portions of the angiographically defined CNV area had no corresponding RPE elevation on OCT (i.e., PED thickness and volume = 0 at these A-scans), there were no areas of visible PED on OCT (in the region of the CNV) for which occult CNV was not evident on angiography. This concept was easily apparent upon simple inspection of the registered FA and OCT annotations/maps, which demon-

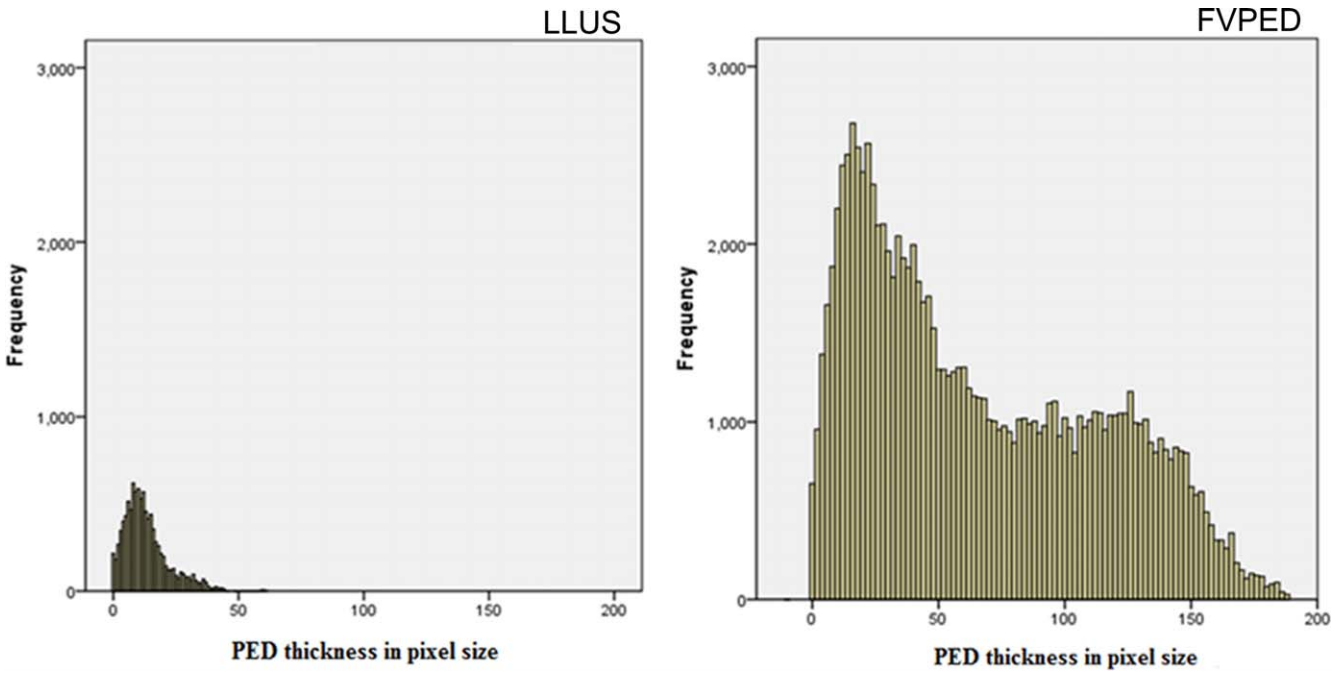

Figure 5. Frequency histograms of distribution of optical coherence tomographic PED thicknesses (in pixels) for all A-scans within FA-determined areas of LLUS and FVPED, respectively. The thickness of regions of LLUS almost never exceeded 50 pixels.

Investigative Ophthalmology & Visual Science

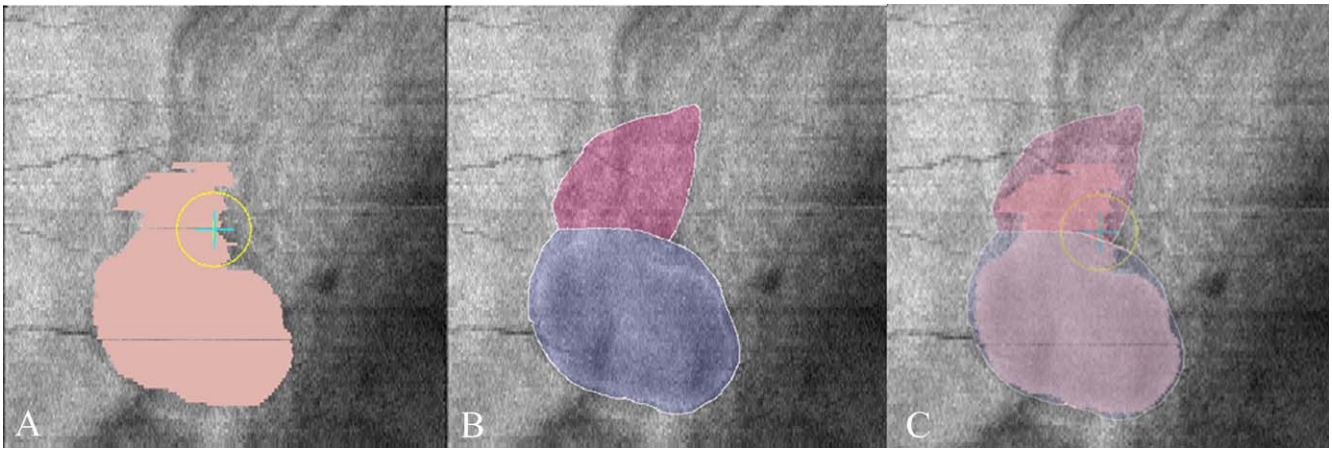

FIGURE 6. Comparison of OCT- and FA-determined occult CNV lesions. (**A**) An OCT projection image with the area of the PED as determined by manual segmentation of the underlying B-scans shaded in *pink*. The foveal center is marked with a *blue cross*. (**B**) The registered FA annotation on the same OCT projection image. *Purple* denotes the areas of fibrovascular PED by FA, and *magenta* corresponds to areas of LLUS as outlined by the grader. (**C**) The merged image with the results of both OCT and FA segmentation shown on the same OCT projection image. Note that the area of the lesion as defined by FA extends beyond the borders of the OCT-defined lesion.

strated that the OCT PED thickness map never extended beyond the borders of the occult CNV area on the FA (Fig. 6).

In addition to thickness, the mean ODRs within the PED of FVPED and that of LLUS were compared. The mean ODR of OCT-evident PED was greater in areas of LLUS (0.24 ± 0.07) compared to areas of FVPED (0.12 ± 0.11), and the difference was statistically significant ($P = 0.03$).

Using the qualitative RPE disruption scale, the RPE was intact or only questionably disrupted in most eyes. Specifically, in LLUS areas (among the 14 eyes that had areas of LLUS), 6 (43%) were graded as normal, 3 (22%) as questionably disrupted, 4 (28%) as mildly disrupted, and 1 (7%) as moderately disrupted. In FVPED areas (among the 10 eyes that had areas of FVPED), 5 (50%) were graded as normal, 2 (20%) as questionably disrupted, 1 (10%) as mildly disrupted, and 1 (10%) as moderately disrupted. There was no statistically significant difference between LLUS and FVPED in terms of RPE integrity ($P = 0.33$ χ^2). The agreement between graders for assessment of RPE integrity was excellent, with a κ of 0.83 (95% CI: 0.73–0.94).

DISCUSSION

In this study, we present the OCT correlates of two specific angiographic subtypes of occult CNV, namely, LLUS and FVPED. Although OCT has progressively supplanted FA as the key modality in the evaluation and management of neovascular AMD, for most clinicians angiography remains essential to confirm an initial diagnosis of CNV and is an important adjunctive tool for retreatment decisions in equivocal cases. In the era of anti-VEGF (vascular endothelial growth factor) therapy, classifying the specific angiographic subtype of CNV has become less important, although Ladas et al.[7] suggested that identifying FVPEDs was of prognostic importance in eyes undergoing photodynamic therapy. Recognizing that these subtypes indicate the presence of CNV, however, remains important, particularly in cases with only subtle LLUS, which may be a challenge to identify. In addition, although the angiographic subtype may not modulate the anti-VEGF therapeutic response, it is certainly possible that OCT-defined components of CNV lesions might respond differently to treatment and that the features of these lesions could have prognostic value. For example, we have demonstrated in both retrospective[8] and prospective[9] studies that the presence of hyperreflective material in the subretinal space may portend a worse visual outcome. These observations highlight the need to better understand the pathophysiology of CNV lesions; and multimodal correlative studies may be of value.

Many groups, including ours, have correlated angiography with OCT to better understand the features of the CNV lesion on OCT.[2] Most investigators now agree that occult CNV generally corresponds to fibrovascular infiltration beneath the RPE; but the differences between LLUS and FVPED have not been previously elucidated. In the present study, we observed that the most striking difference between these subtypes of occult CNV was the thickness of the RPE elevation, with areas of FVPED on average measuring five times thicker than areas of LLUS. This difference would appear to explain many of the clinical and angiographic differences between these lesion subtypes. For example, whereas the borders of FVPED can be well demarcated, LLUS is always poorly demarcated. This is predictable from the OCT characteristics, since it would likely be difficult to discriminate areas of shallower RPE elevation from the surrounding RPE baseline. Similarly, areas of shallow RPE elevation would contain fewer vessels and fewer fluorescein molecules and thus would likely be less bright and slower to become visible until sufficient dye leakage and accumulation had occurred.

Although the difference in PED thickness appeared to be the most dramatic difference between areas of FVPED and LLUS, these lesions also differed in terms of their normalized internal reflectivity, with areas of LLUS having a greater mean internal brightness than areas of FVPED. Subsequent qualitative inspection of these cases demonstrated that areas of FVPED often contained areas of hyporeflectivity believed to correspond to pockets of fluid. We suspect that these dark pockets contribute to the lower mean internal brightness of these lesions. It is possible that accumulation of fluorescein dye in these fluid pockets could result in a brighter, more easily discernible lesion on FA. The integrity of the RPE band on OCT, however, did not differ between these lesion subtypes. Inspection of the RPE status is important as it can significantly impact the angiographic appearance of a lesion; and disrupted RPE can lead to early transmission hyperfluorescence. It should be noted, however, that the absence of discontinuities in the RPE band on OCT does not mean that the RPE is not

Investigative Ophthalmology & Visual Science

depigmented; and such depigmentation could still lead to hyperfluorescence on FA.

Another interesting observation from our analysis is that the angiographic occult CNV lesion was generally larger than the area of RPE elevation noted on the OCT-derived PED thickness map. Since the grading protocol for CNV lesions (adapted from the Macular Photocoagulation Study[10]) requires that the borders of the occult component of a CNV lesion be drawn in the late phases of the FA, we would speculate that the most likely explanation for this apparent discrepancy is the inclusion of lateral fluorescein dye leakage as part of the angiographic CNV lesion.

Our study has many limitations that are worth considering. First, the study was retrospective in nature and thus subject to confounders such as ascertainment bias. Second, because of the relatively small study cohort, the study was not powered to detect small differences in RPE integrity between the occult CNV subtypes. On the other hand, the study was sufficiently powered to illustrate the large difference in PED thickness between LLUS and FVPED, the main parameter under evaluation. While we would have been enthusiastic to include more cases, detailed manual segmentation of RPE elevations in all B-scans in dense OCT datasets can be exhausting and tedious. Our observations could be useful in supporting future larger confirmative studies utilizing automated vascularized PED segmentation and multimodal registration.

Our study also has several strengths, including the use of expert reading center graders, detailed manual segmentation of dense OCT datasets, and consideration of novel parameters such as normalized internal PED reflectivity.

In summary, by detailed segmentation and point-to-point correlation of SD-OCT and angiographic data from eyes with occult CNV, we were able to demonstrate that the most striking difference between LLUS and FVPED is the height of the RPE elevation. These findings may be of benefit in furthering the development of OCT classification systems for CNV lesions for use in clinical trials and clinical practice.

Acknowledgments

Supported in part by the Beckman Institute for Macular Research and a Research to Prevent Blindness Physician Scientist Award.

Disclosure: **A. Hariri**, None; **F.M. Heussen**, None; **M.G. Nittala**, None; **S.R. Sadda**, Carl Zeiss Meditec (F, C), Allergan (F, C), Genentech (F, C), Optos (F, C), Optovue, Inc. (F, C), Heidelberg Engineering (S), P

References

1. Lim JL. *Age-Related Macular Degeneration*. 2nd ed. New York, NY: Informa Health Care; 2008:135–137.
2. Sadda SR, Liakopoulos S, Keane PA, et al. Relationship between angiographic and optical coherence tomographic (OCT) parameters for quantifying choroidal neovascular lesions. *Graefes Arch Clin Exp Ophthalmol*. 2010;248:175–184.
3. Joeres S, Tsong JW, Updike PG, et al. Reproducibility of quantitative optical coherence tomography subanalysis in neovascular age-related macular degeneration. *Invest Ophthalmol Vis Sci*. 2007;48:4300–4307.
4. Chakravarthy U, Walsh AC, Muldrew A, Updike PG, Barbour T, Sadda SR. Quantitative fluorescein angiographic analysis of choroidal neovascular membranes: validation and correlation with visual function. *Invest Ophthalmol Vis Sci*. 2007;48:349–354.
5. Sadda SR, Joeres S, Wu Z, et al. Error correction and quantitative subanalysis of optical coherence tomography data using computer-assisted grading. *Invest Ophthalmol Vis Sci*. 2007;48:839–848.
6. Lee SY, Stetson PF, Ruiz-Garcia H, Heussen FM, Sadda SR. Automated characterization of pigment epithelial detachment by optical coherence tomography. *Invest Ophthalmol Vis Sci*. 2012;53:164–170.
7. Ladas ID, Kotsolis AI, Rouvas AA, Brouzas D, Moschos MM. Efficacy of photodynamic therapy in the management of occult choroidal neovascularization associated with serous pigment epithelium detachment. *Ophthalmologica*. 2007;221:313–319.
8. Keane PA, Liakopoulos S, Chang KT, et al. Relationship between optical coherence tomography retinal parameters and visual acuity in neovascular age-related macular degeneration. *Ophthalmology*. 2008;115:2206–2214.
9. Keane PA, Patel PJ, Ouyang Y, et al. Effects of retinal morphology on contrast sensitivity and reading ability in neovascular age-related macular degeneration. *Invest Ophthalmol Vis Sci*. 2010;51:5431–5437.
10. Fine SL. Macular photocoagulation study. *Arch Ophthalmol*. 1980;98:832.

Investigative Ophthalmology & Visual Science